The American Journal of Human Genetics, Volume *101*

Supplemental Data

CDK10 Mutations in Humans and Mice Cause Severe Growth Retardation, Spine Malformations, and Developmental Delays

Christian Windpassinger, Juliette Piard, Carine Bonnard, Majid Alfadhel, Shuhui Lim, Xavier Bisteau, Stéphane Blouin, Nur'Ain B. Ali, Alvin Yu Jin Ng, Hao Lu, Sumanty Tohari, S. Zakiah A. Talib, Noémi van Hul, Matias J. Caldez, Lionel Van Maldergem, Gökhan Yigit, Hülya Kayserili, Sameh A. Youssef, Vincenzo Coppola, Alain de Bruin, Lino Tessarollo, Hyungwon Choi, Verena Rupp, Katharina Roetzer, Paul Roschger, Klaus Klaushofer, Janine Altmüller, Sudipto Roy, Byrappa Venkatesh, Rudolf Ganger, Franz Grill, Farid Ben Chehida, Bernd Wollnik, Umut Altunoglu, Ali Al Kaissi, Bruno Reversade, and Philipp Kaldis

Supplemental Note: Case Reports

We report here the clinical, genetic and molecular aetiology of a previously unidentified syndrome in individuals with mutations in *CDK10* (MIM:603464).

In Family 1, two affected male siblings were born to Tunisian consanguineous healthy parents. The proband (F1-II:1) was a six year old male child who was referred because of torticollis. He was born to a 28 years old woman and 32 years old first cousin man after full term gestation. At birth, he was hypotonic, displayed intrauterine growth retardation and his subsequent course of development has been of severe retardation in all aspects of development. Extreme hypotonia and profound muscular weakness suggested the diagnosis of a neuromuscular disease, which was not confirmed by tests. Clinical examination of the proband revealed short stature (-4SD), large head (50th percentile) in comparison to his small body. In addition to persistent torticollis, he presented with craniofacial anomalies including synophrys, hypertelorism, ptosis, narrow forehead, depressed nasal bridge, large bulky nose, long philtrum, along with a thin upper lip (Figure 1B, Table 1, and Table S1). To understand the aetiology behind the persistent torticollis, we performed 3D reconstruction CT scans which indicated incomplete development of the posterior arches of the atlas (clefting-arrow) and fusion of the left posterior arch of the atlas with the body of the axis indicative of a massive upper cervical malsegmentation (Figure 1D).

Under the assumption of an autosomal recessive inheritance both affected brothers were investigated for shared homozygosity-by-descent (HBD) regions. Using Affymetrix GeneChip Human Mapping 250K NspI array data and the dCHIP software, we were able to identify a ~5 Mbp HBD region on the very distal part of chromosome 16 (data not shown). Subsequent whole exome sequencing revealed the presence of a homozygous splice site mutation c.609-1G>A (NM_052988.4) disrupting the splice acceptor site of intron 8 of *CDK10* in the affected family members (Figure 1A, 1G, and S1), which is present in a heterozygous state in the tested mother. This mutation (rs767176610, dbSNP) has an allele frequency of 2.488e-05 and has not been found before in a homozygous state (ExAC database).

In Family 2, two affected male siblings were born to Algerian first cousins (Figure 1A). The oldest one (F2-II:4) had intrauterine growth retardation. A neonatal respiratory distress and two episodes of seizures at day 4 were observed. His developmental milestones were severely delayed; he walked independently at 30 months and had language delay. His learning disorders required special education. Examination at 7 years indicated growth retardation (-2.5 SD),

normal occipitofrontal head circumference (OFC), a wide-based gait, a sacral dimple, deep palmar creases, and facial dysmorphism including a triangular face, telecanthus, downslanting palpebral fissures, bilateral epicanthal folds, low-set and posteriorly rotated ears, a small chin, and a nevus flammeus of the glabellar region. Brain MRI and cardiac ultrasound were normal (Table 1, Table S1). By 3D reconstruction CT scan, multilayered spinal segmentation defects were observed: C1 anterior clefting, C2-C3 posterior vertebral bodies fusion with laminae and spinous processes fusion, alongside with sacral S2-S5 posterior clefting. In addition a Th4 hemivertebrae fused with posterior processes of Th3 and Th5 was shown. (Figure 1E, from left to right). His younger brother (F2-II:5) was born after an uneventful pregnancy with normal parameters. Atrial septal defect and pulmonary artery stenosis were diagnosed in the neonatal period. He walked independently at 4 years and had no language. He was also a slow learner requiring special education. Examination at 5 years was similar to that of his brother in many respects; growth retardation (-3 SD), small OFC (-2 SD), wide-based gait, sacral dimple, deep palmar creases, and the same facial appearance. Kidney ultrasounds were normal in both individuals and they had no hearing or visual impairment. Array-CGH analysis with a resolution of 25 kb, revealed a small (2.6-28 kb) homozygous microdeletion of 16q24.3 encompassing exons 2 and 3 of *CDK10*, designated ISCN 2009: arr 16q24.3 89,754,790 -89,757,400 x 0 (hg19) in the two affected individuals (Figure 1G). Quantitative PCR (qPCR) analysis confirmed the 16q24.3 microdeletion (data not shown). Segregation analysis indicated the presence of the deletion in the heterozygous state in the parents and three healthy siblings of the index cases (Figure 1A).

Family 3 is a Saudi family with one affected child (F3-II:2) and one healthy sibling born to consanguineous parents. The proband was referred for evaluation due to severe hydrocephalus with dilated ventricles, thinning of the corpus callosum, and absence of the septum pellucidum, which was diagnosed antenatally by ultrasound. At birth she was hypotonic with marked hydrocephalus, dysmorphic features, and a sacral dimple. Birth weight was 2.9 kg (-1 SD). Brain and whole spine MRI confirmed the diagnosis of supratentorial hydrocephalus with partial agenesis of the corpus callosum and normal spine. Further radiological investigations indicated bilateral nephrocalcinosis and a small atrial septal defect. Later, the individual had recurrent attacks of chest infection demanding recurrent pediatric intensive care unit (PICU) admissions. At 18 months of age she was referred to the genetic facility for further investigations with a length 75 cm (-1.3 SD), weight 8.4 kg (-0.2 SD) and head circumference at 50 cm (3 SD). She had dysmorphic features; high arched palate, brachycephaly, synophrys, low set ears, and broad forehead in addition to the marked hydrocephalus. Detailed metabolic workup was requested including plasma amino acids, urine organic acids and very long chain fatty acids but were all

within normal limits. Currently the individual is 40 months old and started to walk independently. She underwent ventriculoperitoneal shunt insertion and developed seizure, which was well controlled with antiepileptic medications. Karyotyping was normal and CGH microarray indicated homozygosity blocks and no pathogenic changes. Whole exome sequencing was requested and revealed a homozygous c.139delG in exon 2 of *CDK10*, resulting in a truncated protein p.Glu47ArgfsTer21. Both parents were heterozygous for the same mutation. This *CDK10* variant is predicted to cause loss of normal protein function either through protein truncation or nonsense-mediated mRNA decay.

Family 4 is a consanguineous family with three affected members from two separate branches (Figure 1A). Two affected siblings from the first branch were referred for evaluation due to similar facial dysmorphisms (Figure 1B), developmental delay, intellectual disability, and congenital hypothyroidism. The index case (F4-II:1) was the first-born child of first cousin parents of Kurdish descent, originating from Southeastern Turkey. Following an uneventful pregnancy, he was born by normal spontaneous cephalic delivery at term, with a birth weight of 2950 gr (-1.1 SD). Hypotonia was noted at birth and he was interned at level I neonatal care on the fourth postnatal day, due to poor sucking, restlessness, and regurgitations. He was diagnosed with congenital hypothyroidism and thyroid replacement therapy was started. Between 12 months and 3 years of age, he was hospitalized nine times due to lower respiratory tract infections and reactive airway. A work-up comprising viral serology, complete blood count, lymphocyte subset analysis, serum immunoglobulin levels, and sweat test showed results within the normal range. The severity of the infections diminished after age three and the family did not report any infections after the age of seven. He had a febrile seizure at the age of 3 years, during a hospital stay due to pneumonia. Electroencephalogram and cranial MRI results were normal at this time. Neurodevelopmental milestones were significantly delayed; he sat without support at 18 months of age, walked independently at 42 months, used first two-word sentences at 4 years of age, and did not have sphincter control until 6 years of age (Table 1, Table S1). At 8 1/2 years of age, his weight was 12.2 kg (-4.7 SD), height 106 cm (-4.4 SD), and OFC 46.5 cm (-4.6 SD). He had a happy demeanor during examination, was cooperative, but had short attention span. Physical evaluation indicated thick, bushy hair, abnormal hair patterning with two hair whorls on the frontal hairline, bilateral epicanthus tarsalis, upslanting palpebral fissures, mild malar rash, wide nasal bridge and ridge, broad nasal tip with short columella, smooth and long philtrum, thin vermilion of upper and lower lips, high and narrow palate, pointed chin, bilaterally low-set, posteriorly rotated ears with angulated helices, prominent antihelix stems, underdeveloped superior crura, and hypoplastic lobules (Figure 1B). He had doughy, mildly hyperextensible skin, hyperextensibility of the elbow joints and small joints of the hand, small hands with total hand

length of 10.5 cm [<3rd centile], bilateral single palmar flexion crease, fifth finger clinodactyly, bilateral pes planus, broad halluces, and dystrophic toenails (Figure 1C). Hands and feet were cold due to peripheral vasomotor disturbance with episodic cutis marmorata and redness. He had a 5x5 cm patch of hypertrichosis localized on the lumbar area and a sacral dimple. Neurologic and systemic examinations were unremarkable except mildly wide based gait. Detailed metabolic screening including urine and plasma amino acids, urine organic acids, total and free carnitine, acylcarnitine, and oligosaccharides yielded no evidence of an inborn error of metabolism. Full skeletal survey showed fusion of the laminae and pedicles of C2 and C3 vertebrae on the posterior aspects, with rudimentary C2-C3 disk space (Figure 1F) but neck rotation was normal in physical re-evaluation. Using left hand radiograph, bone age was determined to be compatible with 6.5 years. Further work-up comprised routine biochemical screening, evaluation of pituitary axis with basal hormone levels, echocardiography, abdominal and renal ultrasound, audiological evaluation, all with normal results. High-resolution array-CGH using NimbleGen 630 K CGH array did not reveal any major chromosomal anomalies.

Sibling F4-II:2, sister to F4-II:1, was born after an uneventful pregnancy via normal spontaneous delivery at 39 weeks of gestation, with a birth weight of 2280 g (-2.2 SD). Hypothyroidism was noted at 4 months of age, necessitating continuous thyroid hormone replacement. Other pituitary deficiencies were ruled out. She was hospitalized eight times due to lower respiratory tract infections between the age 12 months and 5 years. Immunologic workup at 2 years of age, as performed for her affected brother F4-II:1, failed to demonstrate an underlying immune defect. She had a febrile seizure at the age of 4 years but electroencephalogram and cranial MRI findings were normal. Neurodevelopmental milestones were significantly delayed; she sat without support at 20 months of age, walked independently at 35 months, used first two-word sentences at 5 years of age, and did not have sphincter control until the age of 7 (Table 1, Table S1). At 7 years 3 months, her weight was 11.5 kg (-4.2 SD), height 97.5 cm (-4.7 SD), and OFC 46 cm (-4.4 SD). Dysmorphic facial features included thick and woolly hair, midline capillary hemangiomata on the glabella and on the inferior nuchal region, bilateral epicanthus tarsalis and telecanthus, upslanting palpebral fissures, malar rash, wide nasal bridge and ridge, broad nasal tip, smooth and long philtrum, thin upper lip vermilion, high and narrow palate, pointed chin, bilaterally low-set, posteriorly rotated ears with angulated helices, prominent antihelix stems, underdeveloped superior crura, underdeveloped tragi, prominent antitragi, and hypoplastic lobules (Figure 1B). She had easily bruised, doughy skin, hyperextensible small joints of the hand, small hands with total hand length of 10.3 cm [<3rd centile], bilateral fifth finger clinodactyly, diastasis recti with prominent umbilicus, sacral dimple and bilateral broad halluces. Hands and feet were cold with episodic cutis marmorata and

redness. Neurologic and systemic examination was otherwise unremarkable, with no motor weakness or sensory deficit. Denver II developmental test performed at the chronological age of 7 years 3 months suggested gross motor skills compatible with 44 months, fine motor skills with 22 months, personal-social skills with 25 months, and language skills with 36 months. Eye and fundus examination, a routine biochemical screen, detailed metabolic screening, echo-cardiography, abdominal and renal ultrasonography, chromosome analysis at 500-550 band levels revealed normal results. Full skeletal survey indicated the fusion of the posterior elements of the C2 and C3, with underdeveloped vertebral body of atlas, and atlantoaxial instability. Using left hand radiograph, bone age was determined to be compatible with 5 years.

The affected cousin F4-II:3 was not evaluated in the clinics. History, clinical data, and photographs suggested that he was similarly affected as his affected cousins. He was born via normal spontaneous delivery at 38 weeks of gestation, with a birth weight of 3120 g (0.6 SD). At 3 years 9 months, his weight was 10.5 kg (-3.4 SD), height 86 cm (-3.5 SD), and OFC 44 cm (-3.9 SD). His development was markedly delayed, sitting unsupported at 24 months, and walking independently at 40 months of age. By 45 months, he could speak with only a few simple words without word combinations. Photographs revealed dysmorphic facial features similar to his cousins, including capillary hemangioma on the glabella, bilateral telecanthus, upslanting palpebral fissures, mild malar rash, wide nasal bridge and ridge, broad nasal tip, smooth and long philtrum, thin upper lip vermilion, high and narrow palate, pointed chin, and bilaterally low-set, posteriorly rotated ears (Figure 1B), and a sacral dimple. He also was reported to have pes planus, frequent upper airway infections and vasomotor disturbance of hands. Biochemical work-up, cranial MRI and radiographic evaluation of the cervical spine could not be performed.

Under the hypothesis of autosomal recessive inheritance, using whole exome sequencing, a homozygous donor splice-site mutation was identified in the intron 8 of *CDK10* (c.608+1G>A, Figure 1A and 1G). This mutation was not annotated in dbSNP or in the ExAC database and was confirmed by Sanger sequencing and found to be homozygous in the three patients but heterozygous in their parents and unaffected sibling (Figure 1A).

Family 5 is a Turkish family with one affected child and a healthy sibling, and reportedly nonconsanguineous parents originating from the same small village. IUGR was noted by ultrasound at the third trimester, pregnancy was otherwise uncomplicated. He was born by elective caeserean section at 40 weeks of gestation, with a birth weight of 2080 g (-2.4 SD), height and OFC at birth are unknown. He was admitted to the neonatal intensive care unit for 10 days due to respiratory distress, necessitating noninvasive oxygen administration. Echo-cardiography at three months of age, and routine follow up thereafter revealed mild, nonprogressive dilatation of the left ventricle, and mild pulmonary stenosis. At 8 months of age,

a diagnostic workup included routine biochemistry, complete blood count, urinalysis, thyroid hormone levels, sweat test, anti-gliadin and anti-endomysial antibodies, detailed metabolic screening, and abdominal sonography, all with normal results. He underwent orchiopexy due to bilateral undescended testes at the age of 12 months. He was hospitalized due to pneumonia at the age of 24 months, and was diagnosed with gastroesophageal reflux disease during the hospital stay, which ameliorated with medical therapy. Neurodevelopmental milestones were moderately delayed; head control was achieved at two months of age, he sat without support at 11 months, walked at 24 months, used first two-word sentences at 2.5 years, and achieved sphincter control at 4 years. Denver II developmental test performed at the chronological age of 4 years 3 months suggested gross motor skills compatible with 24 months, fine motor skills with 24 months, personal-social skills with 24 months, and language skills with 22 months. Cranial and lumbosacral MRI performed at 3 years of age showed normal structures. At 6 years 6 months of age, he was evaluated in the genetic outpatient clinics. His weight was 14.5 kg (-3.5 SD), height 107 cm (-2.6 SD) and OFC 49.5 cm (-2 SD). Physical evaluation showed dolicocephaly, high forehead, flared eyebrows, hypertelorism, telecanthus, bilateral ptosis, esotropia, convex nasal ridge with mildly broad nasal tip, underdeveloped premaxilla, smooth philtrum, thin vermilion of the upper and lower lips, high palate, tall chin, and bilaterally prominent, low-set, posteriorly-rotated ears with absent superior crura. He had hyperextensibility of the small joints, small hands with bilateral 5^{th} finger clinodactyly, palmoplantar hyperkeratosis, shawl scrotum, and a sacral dimple. He was extremely friendly and gregarious during the examination. Systemic examination was otherwise unremarkable. High-resolution array-CGH using NimbleGen 630 K CGH array showed no pathogenic variations. Next a trio whole-exome sequencing was performed and filtering of variants were carried out using the exome analysis pipeline 'Varbank' of the Cologne Center for Genomics (CCG). The same homozygous *CDK10* exon 8 splice site c.608+1G>A mutation found in family 4 was also present in proband of family 5 suggesting a possible a founder mutation. Both parents were heterozygous carriers of this mutation (Figure 1A).

We suggest to name this previously unrecognized congenital disease as Al Kaissi syndrome.

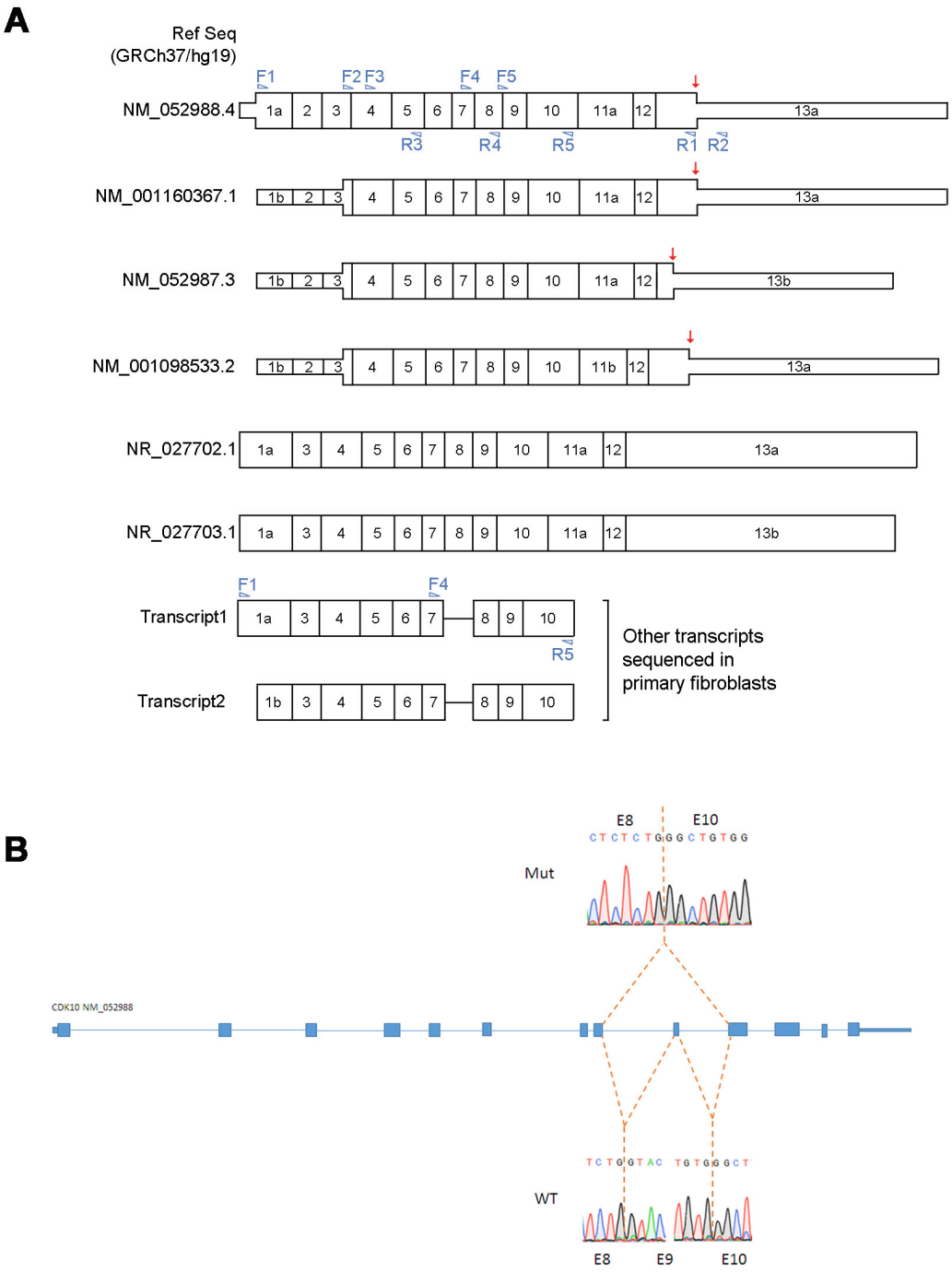

Figure S1: Representation of human Cdk10 transcripts.
(A) Six transcripts for Cdk10 have been described among which 4 are coding (NM_052988, NM_001160367, NM_052987, NM_001098533) and 2 non-coding (NR_027702, NR_027703). Only NM_052988 transcript displays a different start codon for its translation due to a different exon 1; this leads to a longer protein of 360 amino acids due to the translation of a part of the exon 1a, exon 2 and part of the exon 3. Exon 2 and early part of the exon 3 contain the active site of Cdk10 while the cyclin binding motif (PISSLRE) is kept in all transcripts. **(B)** Sequencing of wildtype (WT) and mutant (Mut) transcripts around the exon 8, 9 and 10.

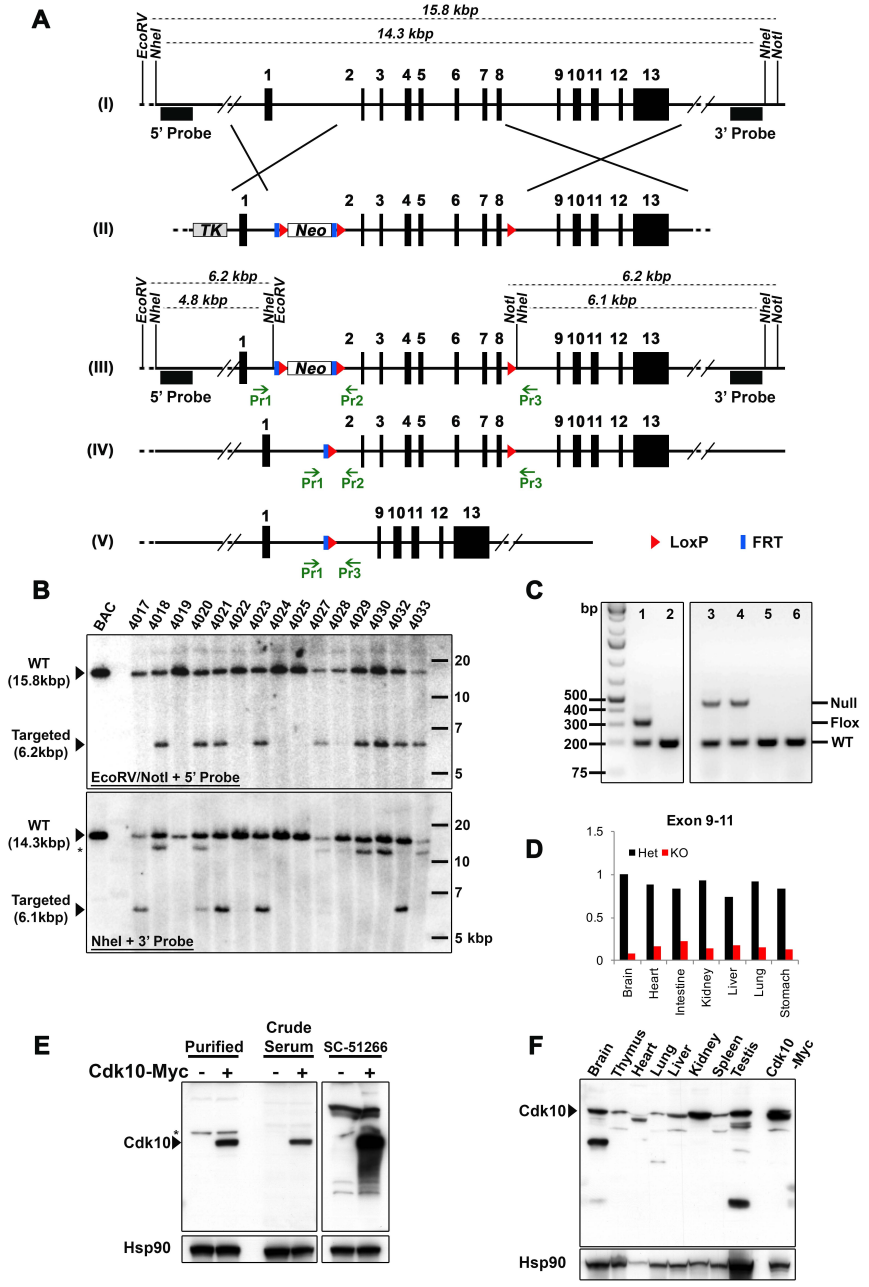

Figure S2: Generation of Cdk10^{flox} mice

(A) To generate Cdk10 knockout, the Cdk10 genomic locus (I, Cdk10^{WT}) was modified in ES cells with the targeting vector (II). A FRT-LoxP-flanked neomycin selection cassette was introduced upstream of exon 2 and a single LoxP recombination site was introduced after exon 8, generating a mutant "Neo" locus (III). Upon expression of FLP recombinase, the neomycin cassette was removed (IV, Cdk10^{Flox}). After Cre recombinase expression, exons 2 to 8 are excised (V, Cdk10^{KO}) resulting in deletion of Cdk10. **(B)** Southern Blotting of selected ES clones after transfection and recombination of the targeting vector. **(C)** Genotyping PCR of obtained different mice harbouring Cdk10^{WT} (WT), Cdk10^{Flox} (Flox) or Cdk10^{KO} (Null) alleles. **(D)** Quantitative RT-PCR of Cdk10 mRNA transcript in different tissues from heterozygous Cdk10$^{WT/KO}$ (Het) and homozygous Cdk10$^{KO/KO}$ (KO) mice. **(E-F)** Immunoblotting of Cdk10 using in house-produced or commercial antibodies on whole cell lysate from non-transfected or transfected NIH3T3 cells **(E)** and from several tissues of Cdk10^{WT} mice **(F)**. HSP90 served as loading control.

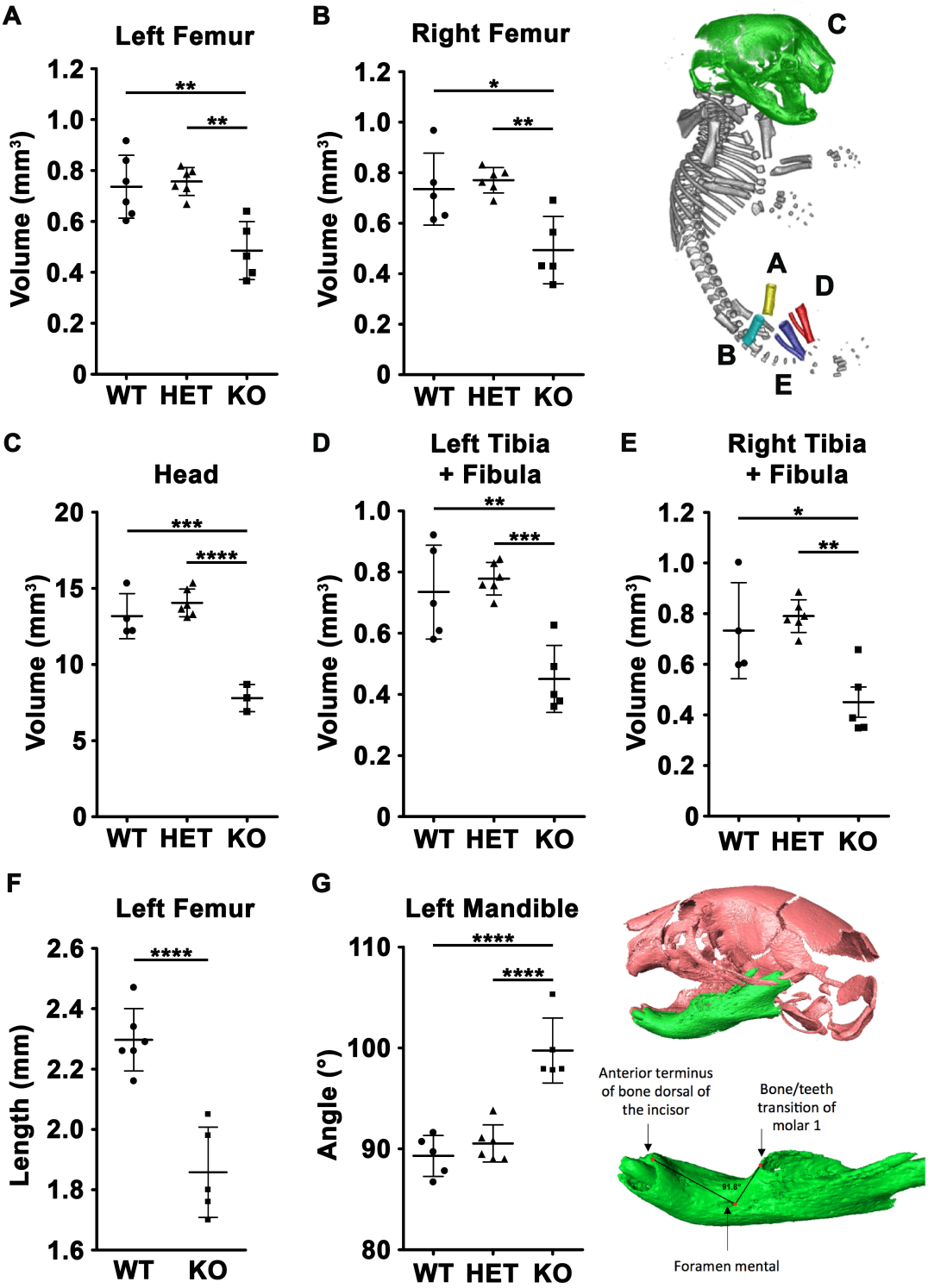

Figure S3: CT scan of mouse skeleton

Measurement of mineralized part from Cdk10$^{WT/WT}$ (WT), heterozygotes Cdk10$^{WT/KO}$ (HET), and knockout Cdk10$^{KO/KO}$ (KO) mice at day P0. Measure of the volume from left **(A)** and right **(B)** femur, the head **(C),** left **(D)** and right **(E)** tibia and fibula. **(F)** Measure of the length of left femur. **(G)** Angle measurement between the anterior terminus of bone dorsal of the incisor, the foramen mental and the bone/teeth transition of molar 1. ANOVA with Tukey's multiple comparison test: * $p<0.05$, ** $p<0.01$, *** $p<0.001$, **** $p<0.0001$. Error bars represent SD.

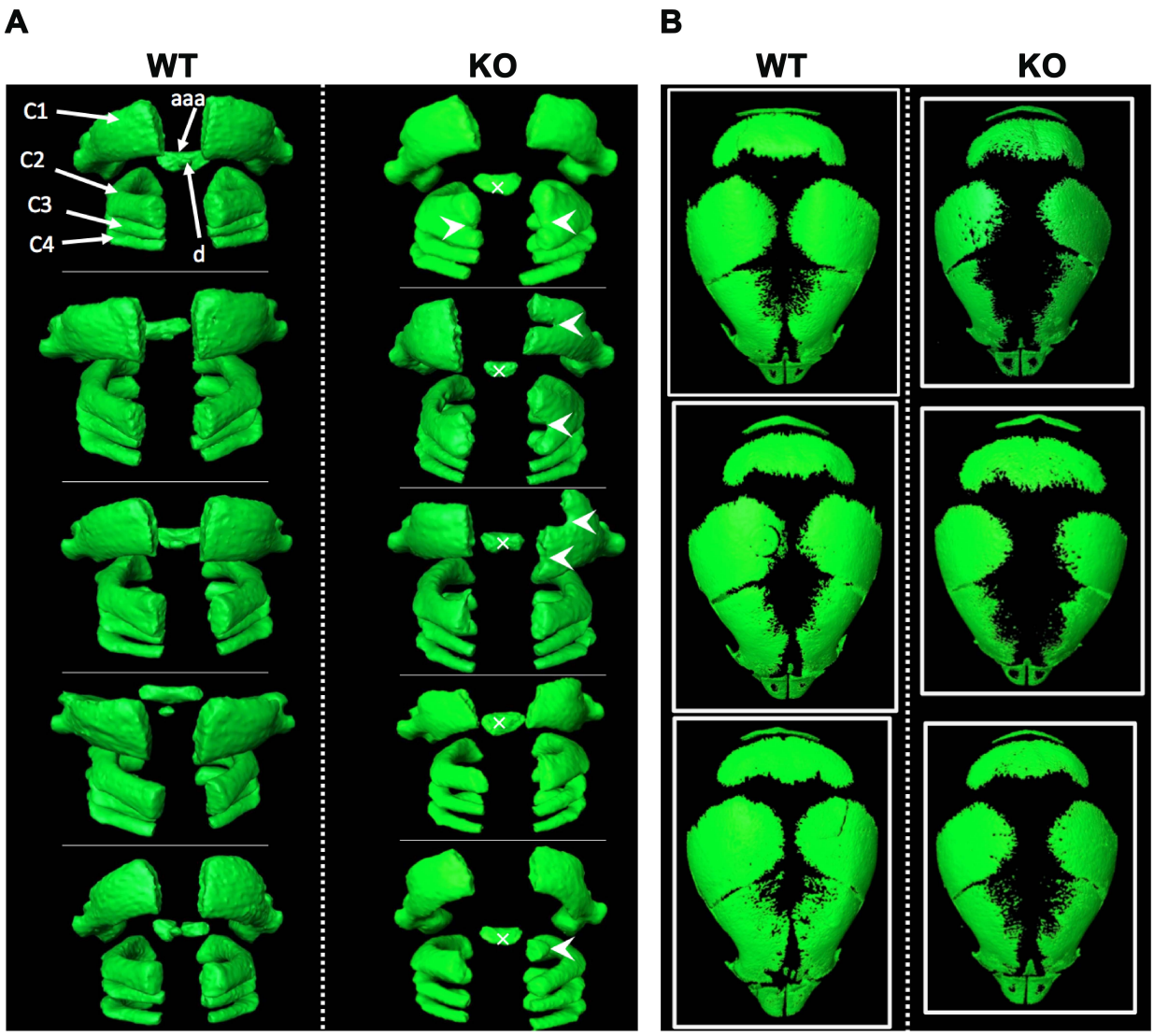

Figure S4: CT scan of vertebrae and skull
(A) Example of posterior 3D visualization of C1 to C4 vertebrae from 5 wild type $Cdk10^{WT/WT}$ (WT) and 5 knockout $Cdk10^{KO/KO}$ (KO) mice. Remarkably, no dens (d) is observed in front of the anterior arch of the atlas (aaa) in the KO animals. The arrows indicate the commonly found bifidity and malsegmentation of the upper cervical vertebral bodies observed in the KO animals. **(B)** Example of skullcap 3D visualization from 3 wild type $Cdk10^{WT/WT}$ (WT) and 3 knockout $Cdk10^{KO/KO}$ (KO) mice. The mineralization of the skullcap appears less accomplished in the KO animals compared to the WT.

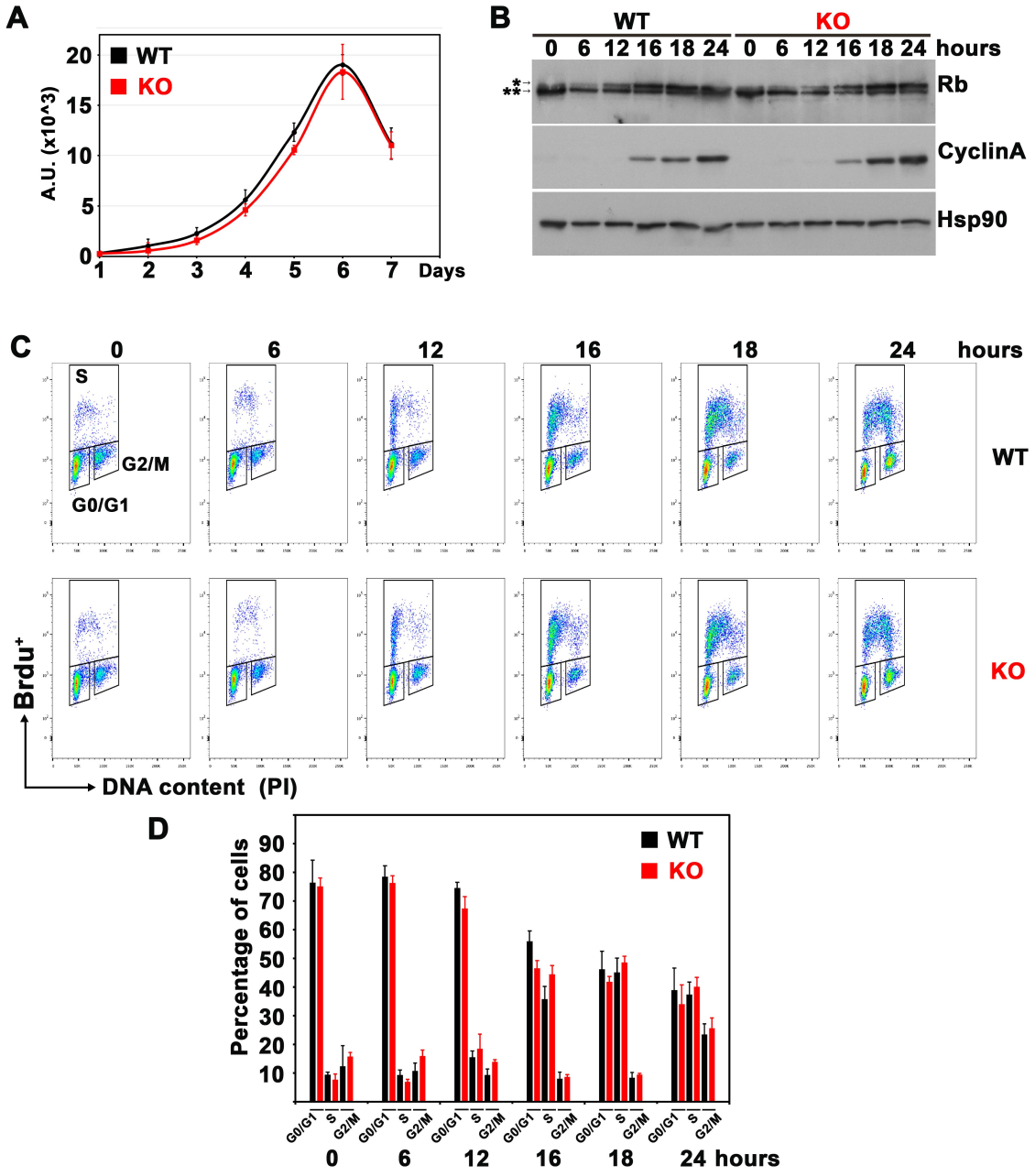

Figure S5: Characterization of Cdk10KO MEFs

(A) Proliferation assay of 3 wild type Cdk10$^{WT/WT}$ (WT) and 3 knockout Cdk10$^{KO/KO}$ (KO) primary MEFs clones. **(B)** Immunoblotting with antibodies against indicated proteins on whole cell lysate from wild type Cdk10$^{WT/WT}$ (WT) and knockout Cdk10$^{KO/KO}$ (KO) primary MEFs collected at different time points after release from serum starvation (G0/G1 synchronization). * and ** indicate hypo- and hyperphosphorylated band of the tumor suppressor Rb, respectively. **(C)** Cdk10$^{WT/WT}$ (WT) and Cdk10$^{KO/KO}$ (KO) MEFs as in (B) were 1hour pulse-labelled with BrdU before collection and analysed by FACS to determine percentage of cells in G0/G1, S, and G2/M phases in a single cell population distributed as BrdU incorporation (BrdU^{+}) versus DNA content (PI). **(D)** Quantitative analysis of 3 wild type Cdk10$^{WT/WT}$ (WT) and 3 knockout Cdk10$^{KO/KO}$ (KO) primary MEFs clones in G0/G1, S, and G2/M phases as represented in (C). Error bars represent SD.

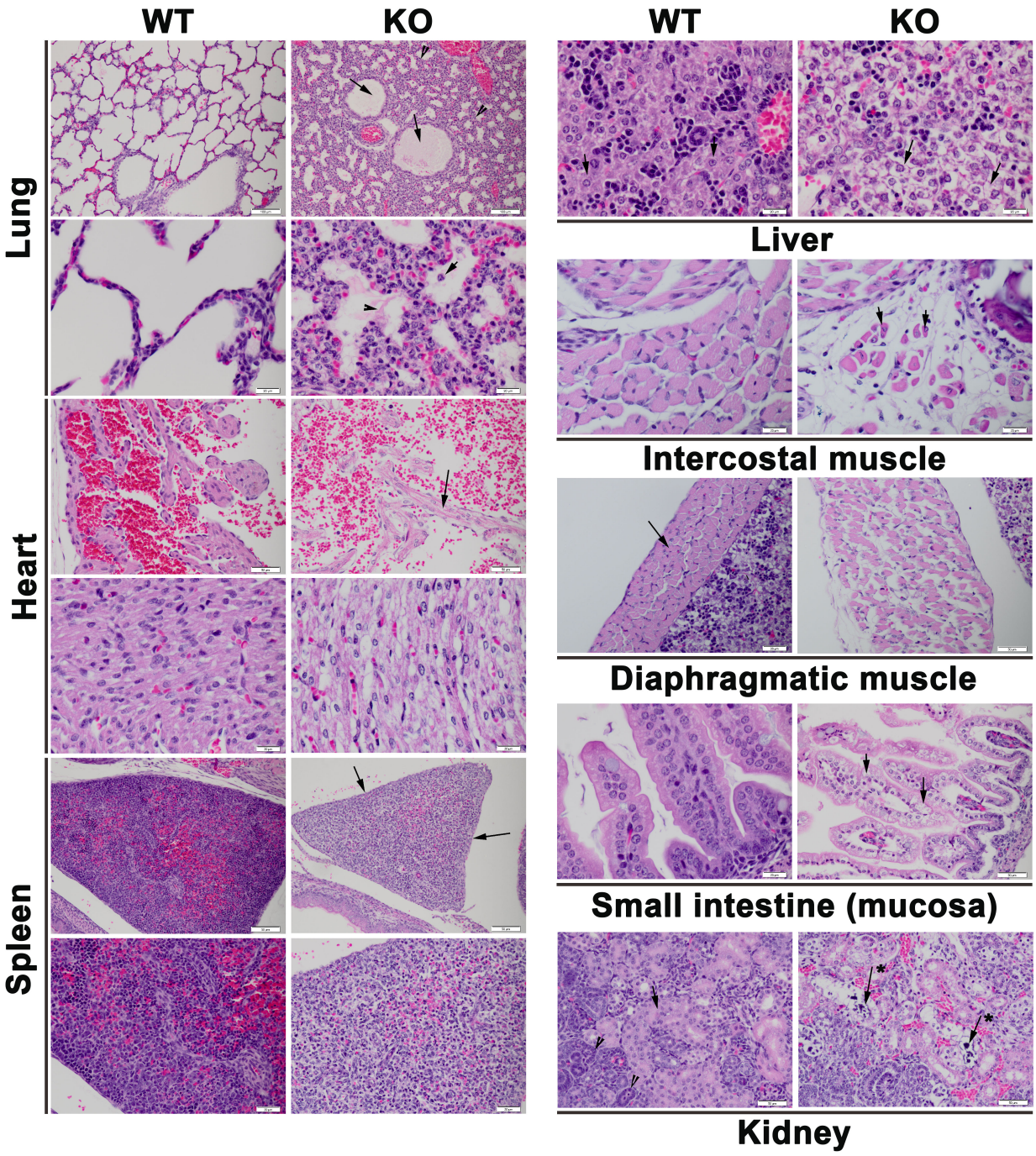

Figure S6: Histology of Cdk10KO mice

H&E stained histological sections of different tissues isolated from wild type $Cdk10^{WT/WT}$ (WT) and knockout $Cdk10^{KO/KO}$ (KO) mice at postnatal day P0.

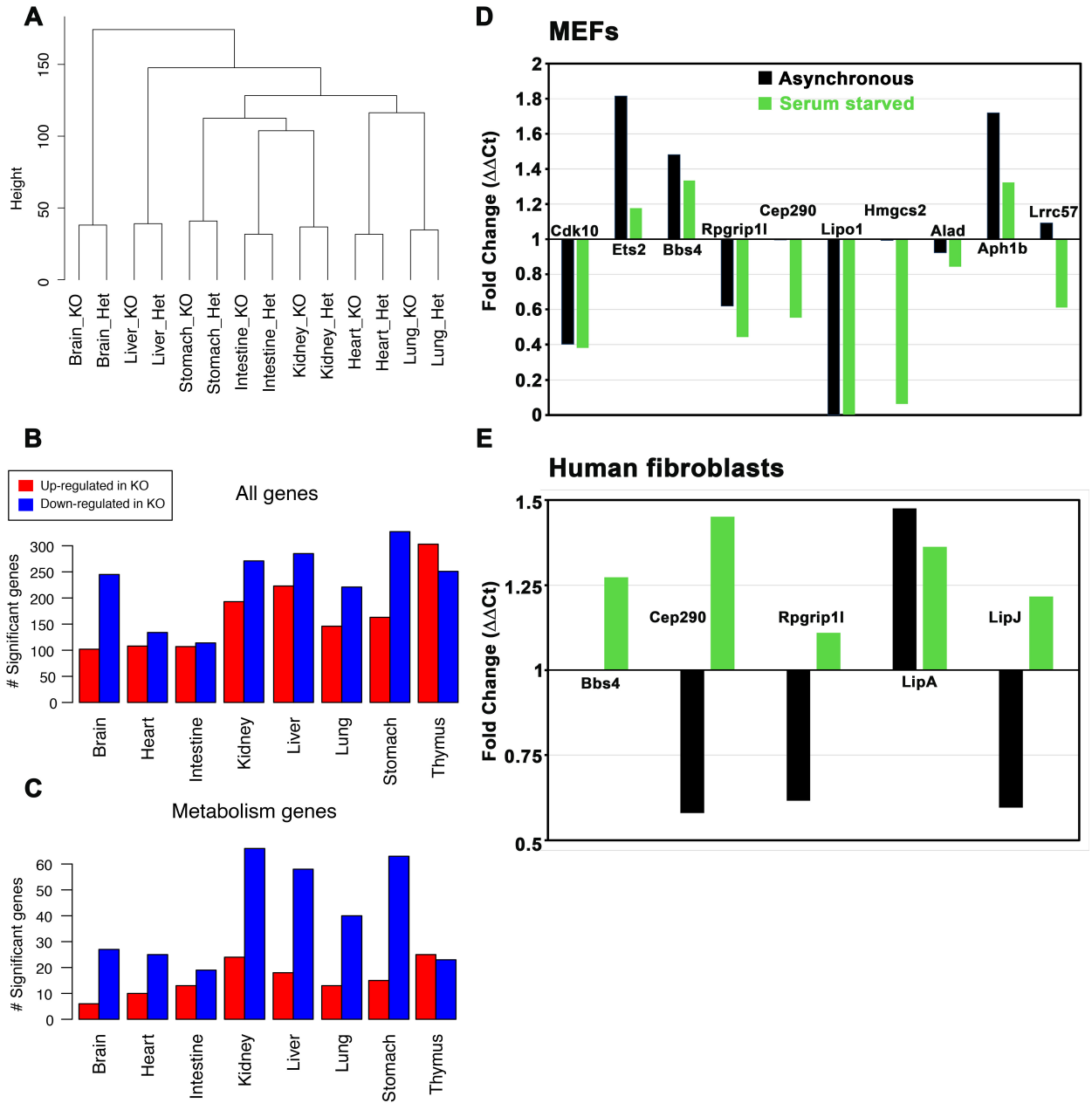

Figure S7: Gene expression analysis of Cdk10KO tissues

(A) Dendrogram of the complete dataset obtained from microarrays of 8 tissues isolated from wild type $Cdk10^{WT/KO}$ (Het) and knockout $Cdk10^{KO/KO}$ (KO) mice at postnatal day P0. **(B-C)** Analysis of the number of genes identified as significantly up- and down-regulated in each tissue in absence of Cdk10. **(D-E)** Quantitative RT-PCR of different transcripts in asynchronous or 96 hours serum starved immortalized MEFs **(D)** or patient-derived fibroblasts **(E).** The bars represent the fold change observed in $Cdk10^{KO/KO}$ (KO) or F4-II:1 individual fibroblasts from the average of 2 primer pairs in comparison to wild type $Cdk10^{WT/WT}$ (WT) or control human fibroblasts after normalization with eEF2 or Gapdh as housekeeping genes using the ΔΔCt method.

Table S5 : Comparison of STAR, BBS and CDK10 syndromes.

	STAR syndrome	*CDK10* syndrome	Bardet-Biedl syndrome
Inheritance pattern	X-linked dominant	autosomal recessive	autosomal recessive
Toe syndactyly	++	-	+
Telecanthus	++	+	-
Anogenital malformations	++	-	++
Renal / urinary tract malformations	++	-	++
Growth retardation	+	++	+
Congenital heart disease	+	+	+
Clinodactyly of 5th finger	+	+	-
Post-axial polydactyly	-	-	++
Dysplastic ears	+	+	-
Hearing loss	+	-	+
Intellectual disability	-	++	++
Cervical spine malformation	-	++	-
Sacral dimple	+	+	-
Obesity	-	-	++
Male hypogonadism	-	-	++
Ocular anomaly	+	-	++ (rod-cone dystrophy)